Pressure swing adsorption for coproduction of power and ultrapure H_2 in an IGCC plant with CO_2 capture

Luca Riboldi[a,1], Olav Bolland[a]

[a]*Energy and Process Engineering Department, the Norwegian University of Science and Technology, NO-7491Trondheim, Norway*

Abstract

The coproduction of power and ultrapure H_2 within an integrated gasification combined cycle (IGCC) plant implementing CO_2 capture offers advantages in terms of flexible operation while retaining good efficiency. The common design includes an absorption unit for removing CO_2 from a high pressure syngas followed by a pressure swing adsorption (PSA) unit for purifying a part of the resulting H_2-rich gas stream. A drawback of this design consists in the necessity for compression of the PSA tail gas in order to recover the energy available in the residual H_2 content. This paper presents two novel configurations for power and H_2 coproduction with CO_2 capture, entirely based on PSA technology. The first relies on two PSA trains in series (*Two-train PSA*), while the other is able to carry out CO_2 separation and H_2 purification within a single PSA train (*One-train PSA*). The two systems were defined and simulated through a composite model of the whole plant. The process simulation results showed that both the configurations proposed are able to shift between the two energy products without compromising the performance of the plant. The load of the plant could be decreased by increasing the ultrapure H_2 throughput, while maintaining a constant feed of coal to the gasifier. The *Two-train PSA* configuration achieved higher performance in terms of energy efficiency and H_2 purity. The *One-train PSA* configuration returned slightly lower but still good performance, while its design includes a single separation stage instead of two. Additionally, both configurations enable the avoidance of PSA tail gas compression giving an advantage against the absorption-based design. A comparative analysis with results taken from the literature seems to confirm this assertion.

Keywords: IGCC, adsorption, flexibility, CO_2 capture, H_2 production, process simulation.

1. Introduction

Two fundamental characteristics for thermal power plants in the near future are the capability of capturing CO_2 in the most efficient way and the possibility to be operated in a flexible manner. For what concerns the CO_2 emissions, the latest IPCC report clearly pointed out that a strong and immediate commitment is needed if we want to limit the potentially devastating effects of global warming [1]. The energy sector is responsible for a large fraction of anthropogenic greenhouse gas emissions [2]. An intervention in this sector has to be undertaken and cannot disregard Carbon Capture and Storage (CCS) [3]. The deployment of other low-carbon energy technologies is also critical, a portfolio of renewable energy sources in the first instance. However, the utilization of fossil fuels is predicted to keep on covering a large share of the power generation in the next decades. CCS allows the exploitation of fossil fuels, while reducing their carbon footprint. Thereby, CCS is an indispensable technology in a

[1] Corresponding author. Tel.: +47 735 93559;
E-mail address: luca.riboldi@ntnu.no

reasonable roadmap towards a carbon constrained world, allowing a smooth transition to a long-term scenario dominated by renewable energies. In this context, the concept of flexible operability becomes of primary importance. With the progressive penetration of renewable energy sources into the energy sector, continuous base load operation mode of fossil fuel power plants will become more and more unlikely [4, 5]. The intermittent nature of some renewable energy sources (e.g. solar and wind) will deeply modify the energy market and, accordingly, the capacity of efficient operation at part-load will become essential for thermal power plants.

Integrated Gasification Combined Cycle (IGCC) seems to be attractive for capturing CO_2 [6]. The high pressure at which the CO_2 separation can be carried out helps limiting the energy penalty. On the other hand, an IGCC plant is not generally suitable for part-load operation. Operating at reduced loads introduces challenges due to the inertia of the process units (mainly air separation unit and gasifier) and to the elevated auxiliary power demand. One way to deal with that could be the coproduction of hydrogen besides power [5, 7]. With the term flexibility in this paper we mean the ability of the plant to shift between two different energy products (i.e. electricity and H_2), resulting from the conversion of a constant coal input, while retaining acceptable efficiency. An IGCC plant which has a variable power-to-hydrogen output may be able, to some extent, to follow the fluctuations in power demand. During low power demand periods, the hydrogen production can be increased to the detriment of the power output. This allows the gasifier and other processing units retaining a working mode close to the design point. The produced ultrapure H_2 can be stored or exported outside the plant. Hydrogen, with certain specifications, is a valuable product for the chemical sector and, possibly, for the transport sector. In this sense, a hydrogen market is predicted to emerge [7, 8].

The common IGCC configuration for hydrogen and power coproduction with CO_2 capture found in the literature consists of: coal gasification, low temperature gas clean-up, sour water-gas shift process, CO_2 removal through an absorption process (normally based on a physical solvent, e.g. Selexol), purification (H_2 purity > 99.9%) of a H_2-rich gas fraction via PSA while the remaining part is fed to a gas turbine. The tail gas from the PSA is compressed and added to the fuel gas stream, given its residual H_2 content. **Figure 1** gives a simplified representation of such system. The fraction of the H_2-rich gas stream depends on the established power-to-hydrogen ratio. The performance attainable by the outlined basic configuration, relying on commercially ready technology, has been extensively analysed in the literature [9-12], also from an economic point of view [8]. Other studies investigated the potential advantages of employing advanced technologies [13, 14] and the possibility of differentiating the fuel mixture to be gasified [13-16]. All the mentioned studies rely on PSA technology for the production of ultrapure H_2. Several PSA designs have been proposed in this sense [17-21]. The main objective of an effective PSA design is to maximize the H_2 recovery, while meeting the required purity specification. A large amount of PSA tail gas would otherwise need to be compressed in order to be fed to the gas turbine and not to waste its energy content. This fuel compression is a complex and energy intensive process. The research for high H_2 recovery has led to increasing complexity of the PSA arrangement. Luberti et al. [22] showed the tradeoff between H_2 recovery and system complexity (productivity accordingly). The aim of the current paper is to address the issue in a different way, which allows for the avoidance of tail gas compression. The idea is to utilize PSA both for the CO_2 separation and for the ultrapure H_2 production. The adoption of the same technology discloses integration opportunities, possibly leading to an efficiency improvement. PSA may be a feasible option for CO_2 capture in coal-fired power plants [23], although absorption seems to generally offer higher overall performance [24]. PSA has also been assessed in a warm gas cleanup arrangement [25] and in sorption enhanced processes [26, 27]. The relative outputs were promising but those PSA systems require tailor-made adsorbent materials and composite processes, whereas this work aims to evaluate common technologies. Provided that, the investigation of possible configurations of PSA-based IGCC plants implementing CO_2 capture while coproducing power and hydrogen is a relatively unexplored topic. A demonstration project at the Valero

refinery in Port Arthur (Texas) [28] applies a dual PSA system, where the main objective is H_2 production with low CO_2 emissions. The produced H_2 is utilized in the manufacturing of petrochemicals and as clean transportation fuel by refinery customers, while the purified and compressed CO_2 is used for enhanced oil recovery (EOR) projects. The PSA system is based on a patented PSA process for simultaneous production of pure H_2 and CO_2 from steam methane reforming syngas [29]. It involves the utilization of two PSA trains consisting of 6 and 3 columns respectively, and the utilization of rotating machinery (i.e., vacuum pumps and CO_2 recycle compressors), which makes it an energy intensive process. A system which is close to what we suggest in the current work has been studied by Chen et al. [13]. The paper discusses the conceptual design and the performance of an advanced IGCC plant using a fixed-bed sorption technology for CO_2 separation [30, 31], while the ultrapure H_2 is produced by a common PSA process. Due to the proprietary nature of the process, not much has been published about it.

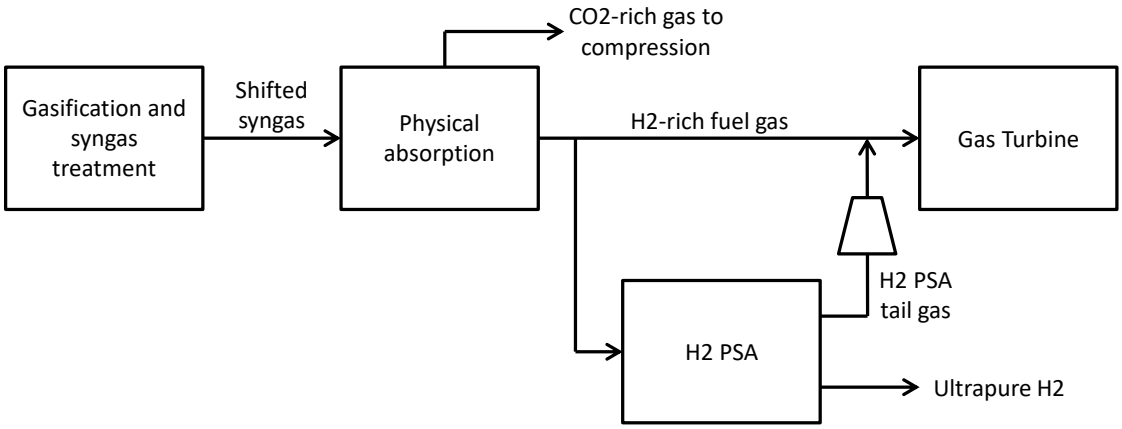

Figure 1. Block flow diagram of an IGCC plant with CO_2 separation by absorption and coproduction of H_2 by PSA.

In this work we investigate, on a system level, two possible configurations for coproduction of power and ultrapure H_2 in an IGCC plant with CO_2 capture. The first one relies on two integrated PSA trains in series: one PSA train with the primary goal of removing and concentrating CO_2 from the shifted syngas, while producing a fuel-grade H_2-rich gas stream; the other PSA train further purifies part of the H_2-rich gas stream in order to meet the specification requirements for being commercialized. The second configuration is based on a single PSA train which is able to separate CO_2, while releasing two H_2-rich gas streams with different H_2 contents. Both configurations studied have been designed with a significant ultrapure H_2 throughput (i.e. up to 14% of the coal lower heating value). The production of ultrapure H_2 was chosen in order to allow comparison with similar works in the literature. However, a design entailing a different throughput would have been likewise possible. Composite models of the defined systems have been built for the process simulations. The composite model includes a dynamic model for the PSA processes and a steady-state model for the other process units (ASU, gasifier, CO_2 compression station, etc.) and for the power island (gas turbine and steam cycle).

2. IGCC plant design and modeling

The analyses of the novel IGGC system configurations are based on process simulations of the entire plant. To enable this approach, a composite model has been build encompassing all the different units constituting the plant. These units can be grouped in the following sections:

- Air separation
- Gasification and syngas treatment

- CO_2 separation and ultrapure H_2 production
- CO_2 compression and flash separation
- Power island

The general layout of the IGCC plant is shown in **Figure 2**. The differences between the two novel configurations proposed are located in the CO_2 separation and ultrapure H_2 production unit. The other sections are common to all the system configurations studied. A description of this common framework is given in the following. When possible, it was based on the set of assumptions defined by the European Benchmarking Task Force (EBTF) [32]. A bituminous Douglas Premium Coal is fed to the gasifier using N_2 as fuel preparation gas. Coal gasification occurs in a Shell-type entrained-flow oxygen-blow gasifier, at a pressure of 44.9 bar. Steam is generated in the gasifier and in the following syngas cooler. The O_2 to be utilized in the gasifier is produced in a cryogenic Air Separation Unit (ASU). The distillation column is operated at 10 bar, producing a 95% pure O_2 gas stream. The ASU is integrated with other units. For instance, 50% of the compressed air entering the ASU is taken from the compressor of the gas turbine. As a byproduct also rather pure N_2 is made available. The surplus N_2 is compressed and used both to convey gas to the gasifier and to dilute the H_2-rich fuel gas to the combustor of the gas turbine. The high temperature syngas (900°C) leaving the gasifier is cooled down (497°C) in a convective syngas cooler and particles removed through wet scrubbers. Syngas is then routed to the Water Gas Shift (WGS) section with a temperature of 178°C. The sour shift process takes place in two consecutive reactors, in order to convert CO to CO_2 and H_2 to the highest possible extent. Steam, coming from the steam cycle, is added to the syngas (with a H_2O/CO ratio of 2) in order to enhance the reaction. The heat of reaction is partially recovered by producing high pressure saturated steam. Alongside the shift process, COS hydrolysis occurs in the WGS reactors. The shifted syngas leaves the WGS section at 235°C and needs to be cooled down to undergo the gas cleaning treatment. It is first cooled against the H_2-rich fuel gas which goes to the gas turbine. The remaining cooling duty is provided by cooling water. During these cooling steps, a large fraction of water still present in the shifted syngas condenses and is extracted. The sulfur compounds have to be removed from the shifted syngas. A single stage Selexol process is applied for H_2S removal. The physical solvent, a dimethyl ether of polyethylene glycol, selectively absorbs H_2S, which is then released during the solvent regeneration. The sulfur-free syngas is routed to the PSA unit. The gas conditions at the entrance of this unit were set to be 38.8 bar and 64°C. PSA is a process based on the utilization of solid adsorbents to selectively retain CO_2 (and, in some instances, other components) from a gas mixture. The regeneration of the column is carried out through a pressure swing operation. In order to assure the operating continuity, a number of columns are set to work in parallel. Each column undergoes the same cycle, which is constituted by a number of proper steps, in a synchronised manner. The exact design of the PSA depends on the configuration considered. Its definition is discussed in dedicated sections of the paper. Three gas streams leave the PSA unit: a CO_2-rich gas stream, an ultrapure H_2 gas stream and a H_2-rich gas stream. The CO_2-rich gas stream is cooled down and sent to the CO_2 compression and flash separation unit, where it is compressed to an appropriate pressure for transportation, i.e. 110 bar. The compression arrangement includes multiple intercooled stages. Since the CO_2 purity obtained by the PSA process is not matching the specification established, a further purification process is implemented and integrated in the CO_2 compression unit. The design of the unit is described in another work [23] along with the advantages and disadvantages of implementing the flash separation [33]. The ultrapure H_2 can be whether commercialized or stocked in order to enhance the flexibility of the plant. Further conditioning processes may be necessary for the delivery of ultrapure H_2 but this has not been considered here. The last product stream from the PSA unit is the H_2-rich gas stream which, after being heated up to about 200°C, is fueling the gas turbine. A dilution with N_2 coming from the ASU is done, mainly in order to be able to use the normal gas turbine combustor designed for natural gas. As rule-of-thumb the N_2 dilution has

been adjusted in the different cases proposed so to retain the same Wobbe index. The gas turbine considered is a large scale F-class, common for all the system configurations studied. The compressed air bled from the compressor is expanded before being sent to the ASU. The air expander increases the total power output by recovering part of the compression work. The flue gas from the turbine is discharged at about 585°C and its remaining energy content is used to produce steam at three different pressure levels in a Heat Recovery Steam Generator (HRSG). Accordingly, the steam bottoming cycle features three pressure levels with reheat, respectively 138 bar, 47 bar and 5 bar. The total gross power output is about 460MW, considering all H_2 for power.

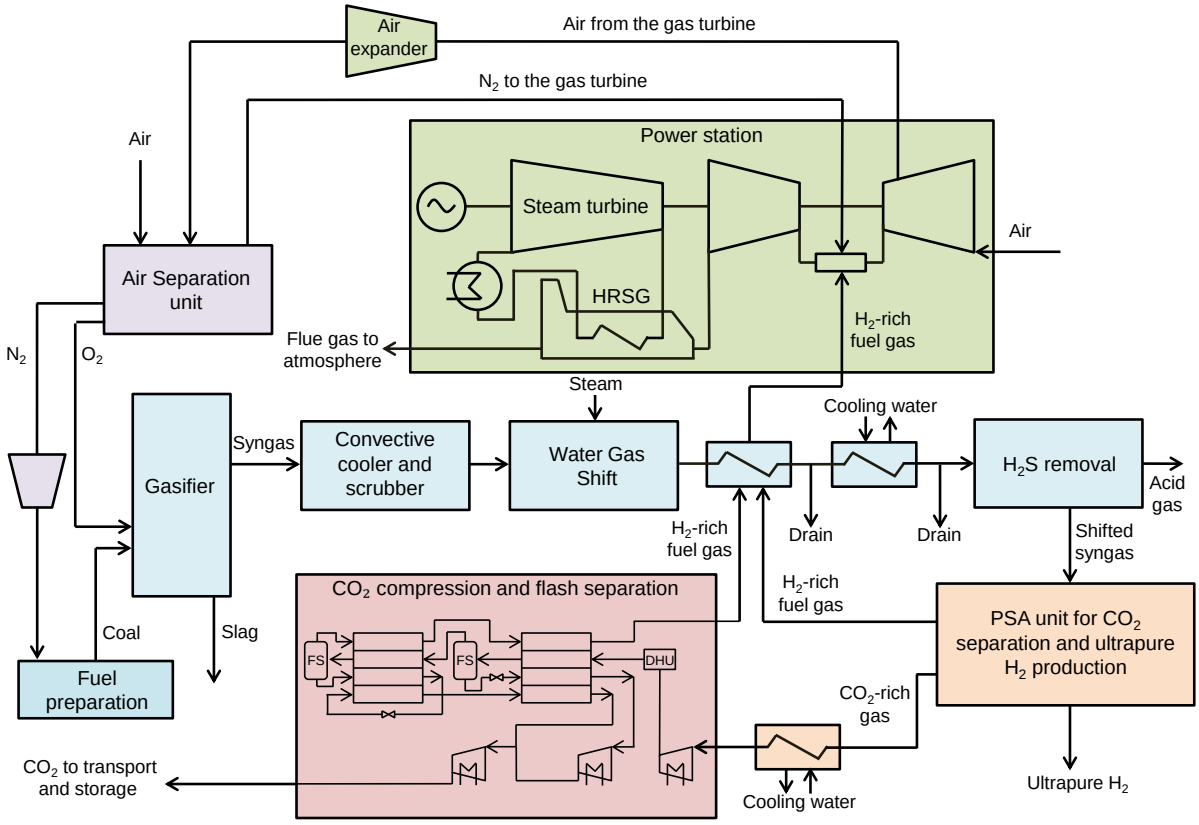

Figure 2. General flowsheet of an IGCC plant coproducing power and ultrapure H_2 with CO_2 capture through PSA.

The air separation, gasification and syngas treatment, CO_2 compression and power island were modeled in Thermoflex (Thermoflow Inc.) [34]. The PSA unit was modeled with gPROMS [35] and a description of the model is provided in the next section. The flash separation process was modeled in Aspen HYSYS [36]. The simulation platforms were set to exchange information through a common Microsoft Excel interface so that an efficient process simulation of the overall plant was made possible.

2.1. PSA model

The dynamic behavior of the adsorption beds constituting a PSA train is described by a 1-dimensional mathematical model with proper boundary conditions for each step of the cycle. The model relies on a set of partial differential and algebraic equations (PDAEs) representing material, energy and momentum balances. For a detailed description of the model, including all the equations adopted, the assumptions introduced and the boundary conditions implemented, reference is made to [23].

Assuming an axially dispersed plug flow, micropore diffusion to be the dominating mass transfer resistance and Linear Driving Force (LDF) approximation to apply, the component and overall material balance equations are, respectively:

$$\frac{\partial C_i}{\partial t}\left[\varepsilon+\varepsilon_p\left(1-\varepsilon\right)\right]=-\frac{\partial\left(u_s C_i\right)}{\partial z}+\frac{\partial}{\partial z}\left(\varepsilon D_{ax,i}\frac{\partial C_i}{\partial z}\right)-\rho_p\left(1-\varepsilon\right)\frac{\partial\overline{q}_i}{\partial t} \tag{1}$$

$$\frac{\partial C_{tot}}{\partial t}\left[\varepsilon+\varepsilon_p\left(1-\varepsilon\right)\right]=-\frac{\partial\left(u_s C_{tot}\right)}{\partial z}-\rho_p\left(1-\varepsilon\right)\sum_i^{NC}\frac{\partial\overline{q}_i}{\partial t} \tag{2}$$

The LDF equation for the adsorption rate is:

$$\frac{\partial\overline{q}_i}{\partial t}=k_{LDF,i}\left(q_i^*-\overline{q}_i\right) \tag{3}$$

The columns are considered to be adiabatic and thermal equilibrium is assumed between the gas and solid phases. The resulting energy balance equation is:

$$\left[C_{v,G}C_{tot}+\frac{\varepsilon_p\left(1-\varepsilon\right)}{\varepsilon}C_{v,G}C_{tot}+\frac{\left(1-\varepsilon\right)}{\varepsilon}C_{p,S}\rho_p+\frac{\left(1-\varepsilon\right)}{\varepsilon}\rho_p\sum_i^{NC}C_{ads,i}\overline{q}_i\right]\frac{\partial T}{\partial t}-\frac{\varepsilon+\varepsilon_p\left(1-\varepsilon\right)}{\varepsilon}RT\frac{\partial C_{tot}}{\partial t}+\frac{u_s}{\varepsilon}C_{p,G}C_{tot}\frac{\partial T}{\partial z}=+$$
$$+\frac{1}{\varepsilon}\frac{\partial}{\partial z}\left(\lambda_{ax}\frac{\partial T}{\partial z}\right)+\rho_p\frac{\left(1-\varepsilon\right)}{\varepsilon}\sum_i^{NC}\left(-\Delta H_{r,i}\right)\frac{\partial\overline{q}_i}{\partial t}$$

(4)

The Ergun equation applies for the momentum balance:

$$\frac{\partial P}{\partial z}=-\left[\frac{150}{d_p^2}\frac{\left(1-\varepsilon\right)^2}{\varepsilon^3}\mu u_s+\frac{1.75}{d_p}\frac{\left(1-\varepsilon\right)}{\varepsilon^3}\rho_G u_s\left|u_s\right|\right] \tag{5}$$

Two adsorbent materials are utilized in the system analyses, with equilibrium parameters and physical properties taken from literature (see **Table 1**), namely an activated carbon [37] and a zeolite 5A [22]. The adsorption equilibrium of different gas components on the activated carbon is described by a multi-site Langmuir model. The equilibria of CO_2, H_2, CH_4, CO and N_2 have been taken into account.

$$\frac{q_i^*}{q_{m,i}}=a_i k_i P_i\left[1-\sum_i^{NC}\left(\frac{q_i^*}{q_{m,i}}\right)\right]^{a_i}\quad\text{, with }\ k_i=k_{\infty,i}\exp\left(-\frac{\Delta H_{r,i}}{RT}\right) \tag{6}$$

For what concerns the zeolite 5A, a dual-site Langmuir model was utilized in order to be consistent with the referenced literature. In this case the gases considered were CO_2, H_2, Ar, CO and N_2.

$$q_i^* = \frac{q_{m,i}^1 k_i^1 P_i}{1+\sum_j^{NC} k_j^1 P_j} + \frac{q_{m,i}^2 k_i^2 P_i}{1+\sum_j^{NC} k_j^2 P_j} \quad \text{, with } k_i^k = k_{\infty,i}^k \exp\left(-\frac{\Delta H_{r,i}^k}{RT}\right) \tag{7}$$

One can notice that while for the activated carbon the CH_4 equilibrium capacity is taken into account, for the zeolite 5A the Ar equilibrium capacity is considered instead. This different approach can be explained by the availability of modelling data and can be justified looking in which part of the system the two adsorbents are applied. Activated carbon is used to process the shifted syngas, where traces of CH_4 are still present. Zeolite is used for the production of ultrapure H_2. In this case the input gas has normally already been purified and the presence of CH_4 is negligible. On the other hand traces of Ar, even though small, can negatively affect the final H_2 purity. Whenever the adsorption equilibria of CH_4 or Ar are not taken into account, their fractions have been included with CO and N_2, respectively.

Table 1. Equilibrium parameters and physical properties of the adsorbents used

Isotherm parameters						
Activated carbon	a	k_∞ (bar^{-1})	q_m (mol/kg)	ΔH_r (kJ/mol)		
CO_2	3,0	2,13E-06	7,86	-29,1		
H_2	1,0	7,69E-06	23,57	-12,8		
CO	2,6	2,68E-06	9,06	-22,6		
N_2	4,0	2,34E-05	5,89	-16,3		
CH_4	3,5	7,92E-06	6,73	-22,7		
Zeolite 5A	k^1_∞ (bar^{-1})	k^2_∞ (bar^{-1})	q^1_m (mol/kg)	q^2_m (mol/kg)	ΔH^1_r (kJ/mol)	ΔH^2_r (kJ/mol)
CO_2	1,08E-07	1,23E-04	0,71	3,71	-38,3	-29,8
H_2	4,23E-07	1,33E-04	0,71	3,71	-19,7	-9,3
CO	2,43E-08	2,32E-05	0,71	3,71	-47,7	-21,0
N_2	2,14E-06	8,99E-05	0,71	3,71	-31,3	-15,0
Ar	1,40E-09	4,90E-04	0,71	3,71	-50,2	-11,2
Physical properties						
	d_p (mm)	ε_p	ρ_p (kg/m3)	$C_{p,s}$ (J/kg/K)		
Activated carbon	2,34	0,57	842	709		
Zeolite 5A	1,70	0,50	1126	920		

Different boundary conditions to the column enable to describe the steps of a PSA process. A single-column approach has been adopted. It consists of modeling a single column of a train, instead of all columns. The cyclic behavior of the PSA process allows this simplification, i.e. all the columns undergoes the same steps cyclically. When two columns of the same train interact, the single-column model relies on the information stored previously during the cycle to describe such interaction. This modeling strategy allows significantly reducing the computational time, without excessive loss in accuracy.

The set of PDAEs was implemented in gPROMS [35]. The Centered Finite Difference Method (CFDM) was used as discretization algorithm for the numerical solution of the model.

Even though its inherent dynamic nature, PSA reaches a condition in which the transient behavior of the entire cycle remains constant and repeats itself invariably from cycle to cycle. This condition is termed Cyclic Steady State (CSS). All the results reported refer to the process at CSS condition.

2.2. Performance indicators and gas stream specifications

This section gives an overview on the performance indicators utilized and on the constraints and specifications considered.
On an energy point of view the assessment of the plant performance is not straightforward, given that two different products have to be considered, i.e. electricity and H_2. Some standards and protocols suggest that different energy products generation efficiencies should be calculated and each referred to the total energy input [38].

$$\eta_{el} = \frac{\text{Net electric output}}{\text{Coal energy}_{LHV}} \tag{8}$$

$$\eta_{H_2} = \frac{\text{Ultrapure } H_2 \text{ energy}_{LVHV}}{\text{Coal energy}_{LHV}} \tag{9}$$

However, we want to define an overall efficiency term which allows an immediate comparison of different systems performances. A first approach suggests to assign a thermal efficiency of 0.6 for the conversion of the exported H_2 beforehand the comparison with power. This value has been chosen referring to a previous work [14] and can be thought to represent the efficiency of a combined cycle for electricity production.

$$\eta_{tot\ 60} = \eta_{el} + 0.6 \cdot \eta_{H_2} \tag{10}$$

Despite the arbitrary choice of the multiplying factor, the so defined cumulative efficiency can be a useful way to compare results from different sources. What we believe to be the most appropriate method of analysis is to discount the H_2 efficiency term with a power production efficiency. This factor takes into account how much of the shifted syngas energy content is converted to power within the same plant configuration under investigation.

$$\eta_{el\ prod} = \frac{\text{Gross electric output}}{\text{Syngas energy input in the gas turbine}_{LHV}} \tag{11}$$

$$\eta^{*}_{tot} = \eta_{el} + \eta_{el\ prod} \cdot \eta_{H_2} \tag{12}$$

In this way it is evaluated how much power could be actually obtained from H_2 if the same efficiency for the energy conversion applies (or other way around, how much power was not produced in order to

obtain H_2). The underlying assumption of this indicator is that the combined cycle (gas turbine and bottoming steam cycle) efficiency would remain constant if all the H_2 was sent to the GT. This is an approximation but it gives reasonable values. The drawback is that there is not always enough information in the literature to calculate the power production efficiency. η^*_{tot} has been computed for all the cases simulated in the current study. For most of the other studies reported there were not enough data available, thus the general comparison between different systems relies on $\eta_{tot\,60}$ as a performance indicator.

The separation performance of all the cases studied considers both the CO_2 and H_2 balance of the system. The effectiveness of CO_2 removal from the syngas is measured in terms of CO_2 recovery, defined as:

$$R_{CO_2} = \frac{\dot{m} \text{ of } CO_2 \text{ compressed for transportation}}{\dot{m} \text{ of } CO_2 \text{ formed throughout the IGCC plant}} \tag{13}$$

In order to better analyse the system, it may be useful to introduce an additional indicator, which still represent CO_2 recovery but taking into consideration only the PSA process. The difference with respect to that above outlined lies in the fact that the processes downstream the PSA are not considered, neither in terms of further CO_2 removal (i.e. the flash separation process) nor in terms of additional CO_2 formed (i.e. the combustion of CO and CH_4 in the gas turbine).

$$PSA-R_{CO_2} = \frac{\dot{m} \text{ of } CO_2 \text{ captured in the PSA process}}{\dot{m} \text{ of } CO_2 \text{ formed upstream the PSA process}} \tag{14}$$

The specifications applying to the different gas streams have been taken from the literature [7, 39]. It must be pointed out that the end application sets the standards for the ultrapure H_2 purity (Y^*_{H2}) and other impurities allowed (in some cases transport and/or intermediate storage actually puts the highest restrictions on H_2 purity but we did not consider this possibility). Proton Exchange Membrane (PEM) fuel cells set the strictest requirements both on H_2 purity (99.99+% vol.) and on the impurities content (to avoid catalyst poisoning). Other applications have more relaxed requirements. When possible we tried to match PEM fuel cell specifications, in order to have the maximum flexibility for the utilization of the H_2 gas stream.
In this work possible additional conditioning processes for the delivery of H_2 have not been taken into account and the H_2 is made available at the pressure and temperature at which it leaves the PSA process.

3. Two-train PSA configuration

Power and ultrapure H_2 are to be coproduced in an IGCC plant by means of PSA. The most obvious way is to take the benchmark configuration as starting point and substitute the absorption unit with a PSA unit. Thereby, the new configuration consists of two PSA trains in series. The motivation behind the investigation of this novel system lies in the integration opportunities that arise from the utilization of the same technology for the CO_2 separation and ultrapure H_2 production. The next section describes the PSA cycles adopted, pinpointing the integration opportunities and explaining how they can be beneficial. The performance of a plant implementing the defined system is following reported and discussed.

The adsorption material selected for the packing of the beds differs between the first and the second train. The first PSA train utilizes activated carbon [37], which demonstrated to provide good CO_2 separation performance at high inlet CO_2 partial pressure [40]. In the second PSA train the focus is no longer on the CO_2 separation but on the H_2 production. Multi-layer structures are often adopted, resulting in an activated carbon layer at the bottom-end of the column and a zeolite layer over it. While the activated carbon is mainly responsible for the uptake of CO_2 and CH_4, the zeolite takes care of the remaining traces of CO and N_2. Ahn et al. [41] demonstrated that gas mixtures rich in N_2 and poor in CO_2 require zeolite-rich beds. Since this is the case in our analysis, a bed completely filled with zeolites has been used. This allows a simplification of the model while the performance is believed to be competitive with the multi-layer counterpart. The zeolite has been selected in the literature [22, 37]. The equilibrium and physical properties of the two adsorbents are reported in **Table 1**.

3.1. *PSA cycles*

The first PSA stage is based on the same cycle already applied in other works [23] for CO_2 separation purposes. It is a 7-bed 12-step cycle operating between a high pressure level of 38.8 bar and a low pressure level of 1 bar. A H_2-rich gas stream is withdrawn at high pressure (38.8 bar) during the adsorption step, whereas a CO_2-rich gas stream is released during the low pressure (1 bar) regeneration steps (i.e. blowdown and purge). The H_2-rich gas stream is then split in two parts: a fraction is fed to the gas turbine combustor; the remaining part is sent to the second PSA for further purification. The second PSA stage is based on a 6-bed 11-step cycle. It has been defined in accordance with the study by Luberti et al. [22], where different advanced PSA cycles to be applied in IGCC plant are defined. The cycle selected for our study is meant to be a compromise between separation performance and complexity of the system. In this second PSA process, whilst the high pressure level is again 38.8 bar at which the ultrapure H_2 is produced, the pressure for bed regeneration is set to 1.8 bar. This has to do with the system integration implemented: the low pressure tail gas of the second PSA process is utilized as purge gas for the first PSA process. Delivering it with a pressure slightly higher than atmospheric allows feeding it to the column of the first PSA train without any compression. Differently than typical system configurations, the tail gas is not utilized as fuel to the gas turbine. The consequent avoidance of tail gas compression is a clear advantage and is made possible by the utilization of PSA as the only gas separation technology. Further, the amount of H_2-rich gas from the second PSA train, which is not sent as fuel to the gas turbine (because is used for purging purposes), is balanced by the additional amount of H_2-rich gas that can be obtained from the first PSA. In fact, the gas stream leaving the adsorption step of the first PSA train is now used only as gas turbine fuel or for producing ultrapure H_2; no fractions of it are any longer recirculated within the cycle as purge gas. The whole system configuration of the *Two-train PSA*, with the different steps undertaken and the scheduling of the cycles, is shown in **Figure 3**. The characteristics of the cycles and of the adsorption reactors have been selected in order to comply with the requirements of the system in the most efficient way possible. Those characteristics are reported in **Table 2**.

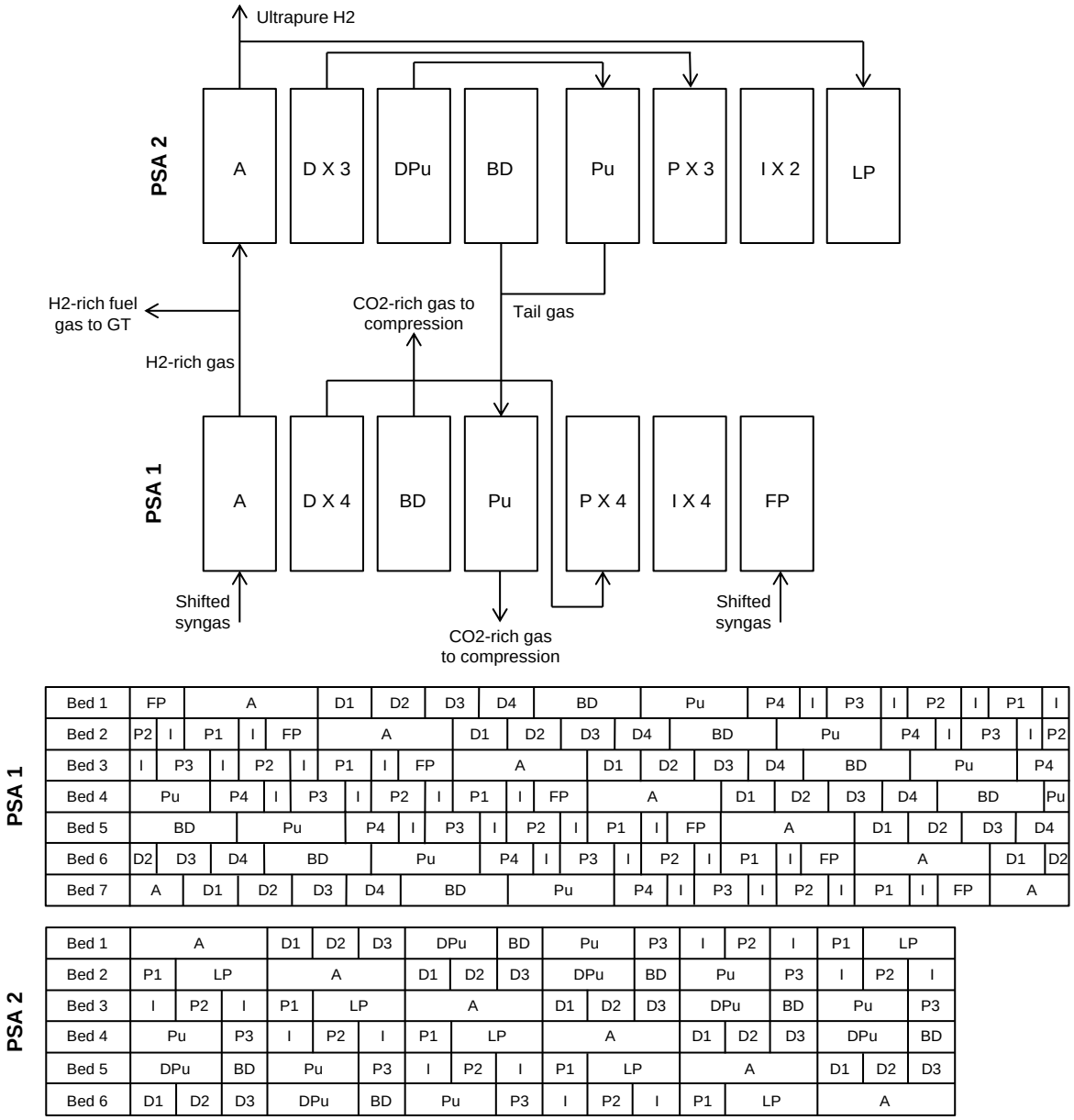

Figure 3. Schematics of the two PSA processes in series. The sequence of the steps undergone by a single column of each train is reported alongside with the scheduling of the cycle. The steps considered are: Adsorption or Feed (A), Pressure equalization - Depressurization (D), Depressurization providing purge (DPu) , Blowdown (BD), Purge (Pu), Pressure equalization - Pressurization (P), Feed Pressurization (FP), Light product Pressurization (LP), Idle (I).

Table 2. Characteristics of the two PSA processes in series and of the adsorption columns.

	Step time (s)									Mole flow rate (mol/s)	
PSA 1	**A**	**D X 4**	**DPu**	**BD**	**Pu**	**P X 4**	**I**	**FP**	**TOT**	**Feed**	**Purge**
	90	41	-	80	59	41	32	41	384	4400	from PSA 2
PSA 2	**A**	**D X 3**	**DPu**	**BD**	**Pu**	**P X 3**	**I**	**LP**	**TOT**	**Feed**	**Purge**
	$t_{cycle2}/6$	$t_{cycle2}/18$	$t_{cycle2}/9$	$t_{cycle2}/18$	$t_{cycle2}/9$	$t_{cycle2}/18$	$t_{cycle2}/9$	$t_{cycle2}/9$	t_{cycle2}	n_{feed2}	200

Bed characteristics			
	L (m)	**D (m)**	**ε**
PSA 1	11	7,1	0,38
PSA 2	10	2,8	0,38

3.2. *Two-train PSA results*

Table 3 summarizes the main outputs of the process simulations. All the cases analysed refer to a common framework with the same coal input to the plant. The gradual shift from power to ultrapure H_2 as outputs of the process has been obtained by modifications of the second PSA cycle. The parameters involved are the scheduling of the cycle (i.e. cycle time steps - t_{cycle2}) and the ratio of H_2-rich syngas sent to the second PSA process out of the total H_2-rich syngas produced by the first PSA process (H_2/Prod). The cases have been termed after the ratio of net electric output and H_2 power output (PW/H_2). Alternative modifications could have been considered to achieve the same effect, e.g. the purge gas flow rate. Changing the share between power and ultrapure H_2 within this system configuration is rather straightforward. High flexibility can be easily achievable without major modifications of the system. According to the cases reported, the load of the plant was varied of about 12% with the process units (ASU, gasification, etc.) working at their design point. Further load changes were not tested but are realistically achievable. The PSA process could be easily designed to deal with a large range of operating conditions, for example accepting lower productivity levels compared to the design proposed here. Thus, PSA does not appear to pose constraints in terms of flexibility. The limiting factor may eventually become the ability of the gas turbine to work at part-load retaining good efficiencies. However, the cases discussed in this section could be handled by the part-load operation strategy of the gas turbine without significant drop in its efficiency.

Table 3. Performance of the IGCC plant implementing the Two-train PSA configuration.

Two-train PSA	**PW/H₂ 2,0**	**PW/H₂ 2,5**	**PW/H₂ 2,7**	**PW/H₂ 3,0**	**PW/H₂ 3,8**
	H_2/Prod 0,249	H_2/Prod 0,224	H_2/Prod 0,214	H_2/Prod 0,204	H_2/Prod 0,188
	t_{cycle2} 342 s	t_{cycle2} 378 s	t_{cycle2} 396 s	t_{cycle2} 414 s	t_{cycle2} 450 s
Coal flow rate (kg/s)	44	44	44	44	44
Coal thermal input (MW)	1095	1095	1095	1095	1095
Gas turbine output (MW)	249	264	266	272	283
Steam turbine output (MW)	166	170	170	172	174
Air expander output (MW)	6	6	6	6	6
Gross electric output (MW)	421	439	442	450	463
Total power consumption (MW)	116	116	115	115	115
Net electric output (MW)	305	324	327	335	348
Net electric efficiency - η_{el} (%)	27,89 %	29,54 %	29,86 %	30,58 %	31,75 %
Power gen. efficiency - $\eta_{el\ prod}$ (%)	64,47 %	64,64 %	64,65 %	64,73 %	64,85 %
CCS					
CO_2 purity - Y_{CO2} (%)	98,8 %	98,8 %	98,8 %	98,8 %	98,8 %
CO_2 recovery - R_{CO2} (%)	86,8 %	86,2 %	85,9 %	85,6 %	85,0 %
Ultrapure H_2					
H_2 throughput (kg/s)	1,28	1,06	1,02	0,93	0,77
H_2 purity - Y^*_{H2} (%)	99,996 %	99,997 %	99,996 %	99,996 %	99,998 %
H_2 thermal power (MW)	154	127	123	111	92
H_2 efficiency- η_{H2} (%)	14,03 %	11,62 %	11,19 %	10,14 %	8,44 %
Overall plant					
Cumulative efficiency$_{60}$ - η_{tot60} (%)	36,31 %	36,51 %	36,58 %	36,67 %	36,82 %
Cumulative efficiency*- η^*_{tot} (%)	36,93 %	37,05 %	37,10 %	37,15 %	37,23 %

For what concerns the energy performance of the new system configuration, some considerations can be argued from the simulations results. Augmenting the throughput of ultrapure H_2 decreases the net electric efficiency. This was expected since a fraction of the coal energy input is stored as chemical energy in the H_2 and, hence, not used for producing power. The energy accumulated in the ultrapure H_2 is accounted for in the H_2 efficiency. The higher the throughput of ultrapure H_2, the higher is that efficiency term. What can be thought to be the real criterion for comparisons for all the cases is one of the cumulative efficiency terms defined. A detailed analysis of the energy balance shows that the system configuration leads to a slight increase of the auxiliary power consumption when the ultrapure H_2 production is increased. This is the result of two opposite effects connected with the two main power consumptions varying in the cases reported:

- The CO_2 compression power.
- The compression power for the N_2 to dilute the fuel in the gas turbine.

For the present configuration and the way to shift from one power product to the other, an increase of ultrapure H_2 throughput implies an increase of CO_2 recovery (PSA-R_{CO2}) and a decrease of CO_2 purity (PSA-Y_{CO2}) in the PSA process. This results in a larger CO_2-rich stream mass flow rate to be compressed and, hence, in more power required. Conversely, when more ultrapure H_2 is produced, necessarily a lower H_2 amount is used as fuel to the gas turbine. The dilution with N_2 is reduced in accordance with the Wobbe index and the power to compress that N_2 stream decreases. The overall effect is a slight increase of the auxiliary power consumption with higher ultrapure H_2 throughput. If the energy content of H_2 is discounted by a factor of 0.6, the outlined situation causes the $\eta_{tot\ 60}$ to decrease when shifting the production on ultrapure H_2. Even if the discounting factor considered is $\eta_{el\ prod}$, which is calculated to be slightly lower than 0.65, the cumulative efficiency decreases with the ultrapure H_2 throughput. The multiplying factor to approximately equalize the energy performance for all the cases reported would be as high as ≈ 0.69. The design point of the plant would preferably be one with a low ultrapure H_2 throughput. Whether the described trend holds for larger variations of the plant products has not been investigated. Additional issues may arise (e.g. performance of the gas turbine at reduced loads).

The performance related to CO_2 separation is not heavily influenced by modifications in the split between power and ultrapure H_2. As previously mentioned, a larger ultrapure H_2 throughput would cause PSA-R_{CO2} to increase and PSA-Y_{CO2} to decrease. On a plant perspective the final Y_{CO2} is rather stable, due to the flash separation process, while R_{CO2} increases slightly mainly due to the higher PSA-R_{CO2}.

4. One-train PSA configuration

This section investigates the possibility of producing ultrapure H_2 as a secondary product stream from a single PSA process, which retains its ability to separate and concentrate CO_2 from a shifted syngas stream. The general design of the novel PSA process is based on a previous work [23]. Some modifications are introduced in the PSA arrangement in order to enable the additional production of ultrapure H_2. No additional separation stages for CO_2 separation and H_2 production have to be included in the system configuration. The bed is assumed to be filled with the same activated carbon used in the *Two-train PSA* configuration [37]. The following sections outline the design of the gas separation unit and analyse the performance of the resulting system.

4.1. *Modified PSA cycle*

The PSA process consists of a 7-bed 13-step cycle operating between a high pressure level of 38.8 bar and a low pressure level of 1 bar. The H_2-rich products are obtained at high pressure (38.8 bar) during the adsorption step. The regeneration is carried out by lowering the pressure down to 1 bar and allows for extracting a CO_2-rich gas stream. The main modification introduced with regard the original cycle is to split the adsorption step in two parts. During the first part (A1) the off-gas will be constituted by ultrapure H_2, while during the second part (A2) it will be the H_2-rich fuel for the gas turbine. For both the steps the feed is the shifted syngas. If the column is sufficiently regenerated, when the syngas is first introduced all the gases other than H_2 get adsorbed in the first part of the bed. Thus, a very high-purity stream of H_2 is leaving the column. Such high H_2 purity for the off-gas stream cannot be kept for long, since soon some impurities begin to breakthrough. When that is the case, the second part of the adsorption step takes over and the off-gas is used as gas turbine fuel. **Figure 4** and **Table 4** give an overview of the modified cycle configuration, showing the sequence of steps undergone by a single column of a train, the cycle scheduling and the characteristics of the adsorption column. Apart from splitting the adsorption step into two parts, other modifications needed to be introduced in comparison to the reference PSA cycle. In the first instance, the continuous and possibly stable feed to the gas turbine had to be ensured. This translates in one of the 7 columns of the train always undergoing the second part of the adsorption step (A2). In order to comply with that, the time length of the first depressurization step (D1) was decreased to allow accommodating the step A1 in the scheduling of the cycle. This countermeasure allowed the A2 steps of the different columns to follow one another in a continuous pattern (see **Figure 4**) and to ensure the continuous feed of the gas turbine. The decrease of the D1 step time implied an equal decrease of the relative pressurization step (P1). One more modification of the PSA cycle is the nature of the purge gas stream. In the cases analysed, part of the ultrapure H_2 is adopted, instead of the H_2-rich gas for the gas turbine. The utilization of ultrapure H_2 was made necessary by the necessity of a significant regeneration of the column, which needs to be free from impurities when the A1 step begins.

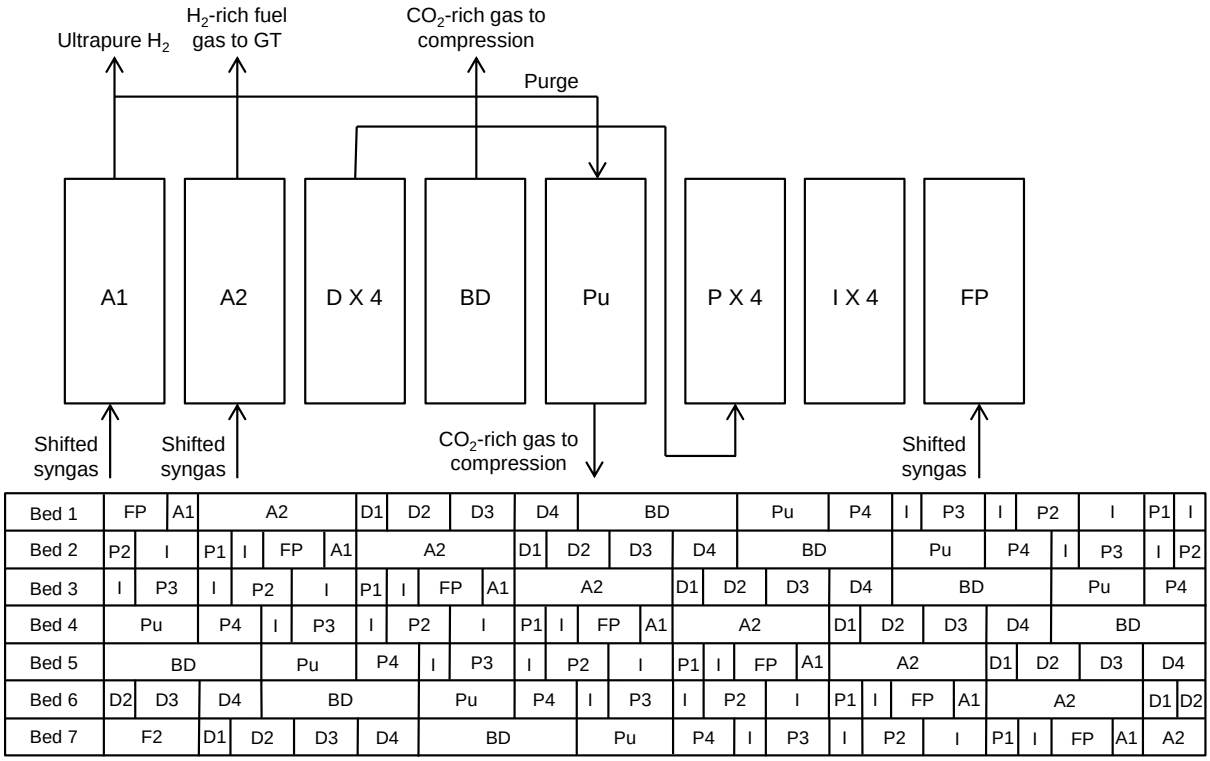

Figure 4. Schematic of the single PSA process. The sequence of the steps undergone by a single column of the train is reported alongside with the scheduling of the cycle. The steps considered are: Adsorption or Feed with ultrapure H_2 production (A1), Adsorption or Feed with fuel-grade H_2 production (A2), Pressure equalization - Depressurization (D), Blowdown (BD), Purge (Pu), Pressure equalization - Pressurization (P), Feed Pressurization (FP), Idle (I).

Table 4. Characteristics of the single PSA process and of the adsorption column.

	Step time (s)											Mole flow rate (mol/s)	
	A1	**A2**	**D1**	**D X 3**	**BD**	**Pu**	**P X 3**	**P1**	**I**	**FP**	**TOT**	**Feed**	**Purge**
PSA	25	90	16	41	80	59	41	16	57	41	630	3490,3	3490,3·P/F

	Bed characteristics		
	L (m)	**D (m)**	**ε**
PSA	12	6,8	0,38

4.2. One-train P*SA results*

Table 5 summarizes the main outputs of the system simulations with coproduction of power and H_2 through a single PSA train. The cases refer to different purge-to-feed (P/F) ratio in the PSA process while the coal input is constant. Modifying the P/F ratio translates in modifications of the purge flow rate applied (since the feed flow rate is kept constant). Such basic procedure enables different splits between power and ultrapure H_2 production. The cases have been termed after the ratio of net electric output and H_2 power output (PW/H_2).

Table 5. Performance of the IGCC plant implementing the One –train PSA configuration.

One-train PSA	**PW/H_2 2.2**	**PW/H_2 2.6**	**PW/H_2 3,0**	**PW/H_2 3,5**	**PW/H_2 4,3**
	P/F 0,09	P/F 0,12	P/F 0,15	P/F 0,18	P/F 0,21
Coal flow rate (kg/s)	43	43	43	43	43
Coal thermal input (MW)	1088	1088	1088	1088	1088
Gas turbine output (MW)	252	261	270	278	287
Steam turbine output (MW)	167	169	171	173	175
Air expander output (MW)	6	6	6	6	6
Gross electric output (MW)	425	436	447	458	468
Total power consumption (MW)	111	113	115	117	119
Net electric output (MW)	314	323	331	340	349
Net electric efficiency - η_{el} (%)	28,85 %	29,66 %	30,46 %	31,28 %	32,07 %
Power gen. efficiency - $\eta_{el\ prod}$ (%)	64,36 %	64,53 %	64,68 %	64,85 %	64,94 %
CCS					
CO_2 purity - Y_{CO2} (%)	98,9 %	98,9 %	99,0 %	99,0 %	99,0 %
CO_2 recovery - R_{CO2} (%)	83,2 %	84,3 %	85,1 %	85,7 %	86,1 %
Ultrapure H_2					
H_2 throughput (kg/s)	1,21	1,06	0,93	0,80	0,68
H_2 purity - Y_{*H2} (%)	99,842 %	99,933 %	99,968 %	99,983 %	99,990 %
H_2 thermal power (MW)	142	126	111	96	81
H_2 efficiency- η_{H2} (%)	13,01 %	11,62 %	10,22 %	8,84 %	7,46 %
Overall plant					
Cumulative efficiency$_{60}$ - η_{tot60} (%)	36,66 %	36,63 %	36,60 %	36,58 %	36,55 %
Cumulative efficiency$_{*}$- η_{*tot} (%)	37,23 %	37,15 %	37,08 %	37,01 %	36,91 %

It has to be pointed out that only one case of those reported matched the set H_2 purity specification, i.e. 99.99+% vol, and this constitutes the biggest drawback of the *One-train PSA* configuration. The case matching the purity specification is that with a P/F ratio of 0.18. Some measures could be taken in the other cases in order to increase the ultrapure H_2 purity, though those would involve a reduction of ultrapure H_2 throughput. The general remark is that there is a trade-off between the ultrapure H_2 purity and throughput. The stricter are the constraints on ultrapure H_2 purity, the less flexible is the operation. If PEM fuel cells are considered as end-application for the produced H_2, this configuration may not be able to cover a large range of power output variations. On the other hand, assuming that lower H_2 purities are acceptable (H_2 used for other end applications or simply stored for allowing flexible operations), a certain degree of flexibility in the power production is possible with minimal modifications in the system, i.e. simply increasing/decreasing the P/F ratio of the PSA process.

Assuming a relaxed specification on H_2 purity applies, the load of the plant was varied of about 10% . The change in the modes of operation did not involve any significant variation in the process units upstream the PSA. Higher load changes are feasible in accordance with reduced H_2 purity requirements and with the capability of the gas turbine to work off-design. A worth-to-mention advantage of this system configuration is that it is designed with a single separation stage for CO_2 separation and H_2 production. Both the benchmark arrangement (absorption unit and PSA unit) and the first configuration

studied in this paper (two PSA trains) necessitate two different separation stages. A single stage translates in reduced footprint and, possibly, capital costs.

From an energy performance perspective, the coproduction of ultrapure H_2 decreases the net electric efficiency and increases the H_2 efficiency. Similarly to the *Two-train PSA* configuration, the two power consumptions undergoing significant variations in the cases analysed are the CO_2 compression power and the compression power for the N_2 to dilute the fuel in the gas turbine. The latter retains the same behaviour previously outlined. Higher ultrapure H_2 throughput means lower H_2 to the gas turbine and lower N_2 dilution needed, which results in decreased compression power. The CO_2 compression power is influenced in a different manner compared to what we discussed before. To increase the ultrapure H_2 throughput the P/F ratio needs to be reduced. Consequently, the purge flow rate diminishes leading to a lower PSA-R_{CO2} and a higher PSA-Y_{CO2}, and, ultimately, to a smaller mass flow rate to be compressed. Thus, the CO_2 compression power consumption decreases with enhanced ultrapure H_2 production. The two effects described act in the same direction, decreasing the power consumption when the ultrapure H_2 throughput increases. The overall result is that both $\eta_{tot\,60}$ and η^*_{tot} tend to increase when shifting the production to ultrapure H_2. The thermodynamic factor equalizing the energy performances in all the cases would be ≈ 0.58, which suggests the plant design point should be one with a significant ultrapure H_2 throughput. As pointed out for the other configuration, the validity of the described trend has not been assessed for a larger range of power output variations.

The performance related to CO_2 separation is similar in all cases. The modifications introduced to the PSA process in order to coproduce H_2, do not hinder significantly the effectiveness of the cycle. The CO_2 purity achieved is stable in a neighborhood of 99%, thanks to the presence of the flash separation process integrated in the CO_2 compression station. The CO_2 recovery undergoes a slight decrease when coproducing ultrapure H_2.

5. Discussion of the results

The novel system configurations demonstrated to entail a high degree of flexibility. Shifting between power and ultrapure H_2 allows for a load-following mode of operation with minimal modifications in the process units. PSA technology demonstrated to be rather effective in this sense. Minimal adjustments in the PSA unit arrangement allowed for obtaining different splits of the product outputs, without any significant impact on the upstream processes. Further, PSA can be easily tuned in accordance to the system requirements giving a high degree of freedom in the design phase. For instance, if the plant was requested to produce a lower amount of ultrapure H_2, both PSA configurations could be designed according to that specification (i.e. different sizes of the column, cycle scheduling, etc.).

Previous studies implemented the coproduction by utilizing a PSA process downstream an absorption unit. Absorption is currently believed to be the most effective and mature technology for CO_2 removal from a shifted syngas, while PSA is the benchmark for H_2 purification. However, an issue connected to this configuration consists in the necessity for a compression of the PSA tail gas. The tail gas has a non-negligible H_2 content which must be recovered. The common practice is to compress the gas stream and feed it to the gas turbine as fuel. The tail gas compression increases the plant power consumption and is the main additional source of energy penalty when implementing ultrapure H_2 coproduction. Both the system configurations proposed in this work enable the avoidance of this tail gas compression. Thereby, it was expected the performance of the system to be enhanced in comparison to the benchmark alternative (i.e. absorption + PSA). With regard to that, some considerations can be drawn by looking at **Table 6**. A premise is necessary before the analysis. A range of different results can be found in the

literature estimating IGCC plant performance. This is due to the various configurations, operating conditions and computational assumptions that can be adopted for these systems. We tried to establish some key assumptions in order to set a common framework for comparison: the set of results chosen from the literature needs to be representative of an IGCC plant as close as possible to the system defined in this paper (and based on EBTF recommendations [32]) and should rely on mature technologies. Furthermore, the plant should be designed to produce power as the primary product, whereas ultrapure H_2 is the byproduct. This last consideration brought us to exclude some studies where the context is overturned (i.e. gasification plant designed for H_2 production with an auxiliary power production). The selected works display performances which are generally lower to what is thought to be the current state-of-the-art, especially in terms of energy efficiency. In a previous work, it was discussed how IGCC plants implementing CO_2 capture through a PSA process is not yet as competitive as the absorption-based counterpart [24]. One main reason behind the relatively low net electrical efficiency displayed by the first work selected [10] is believed to be the gasification technology adopted. A Siemens gasifier with water quench was chosen. The second set of results selected [7] exhibits a more substantial energy penalty. In this case more conservative assumptions seem to have been applied. An example is the adoption of an E-class gas turbine, which results in a significant efficiency reduction compared to the utilization of next generation gas turbines.

*T*able 6. Performance of IGCC plants implementing CO_2 capture either with or without ultrapure H_2 coproduction.

	Coal input	**CO_2 capture**	**R_{CO2}**	**Y_{H2}**	**η_{H2}**	**η_{el}**	**$\eta_{el\ prod}$**	**η_{tot60}**	**η^*_{tot}**
	MW	**technology**	**%**	**%**	**%**	**%**	**%**	**%**	**%**
Only power PSA	971	PSA	84,6	-	-	36,21	64,22	36,21	36,21
Two-train PSA	1095	PSA	85,2	99,998	8,44	31,75	64,85	36,82	37,23
One-train PSA	1088	PSA	85,7	99,983	8,84	31,28	64,85	36,58	37,01
Cormos [10]	1167	Selexol	92,4	-	-	36,02	-	36,02	-
Cormos [10]	1167	Selexol	92,4	99,950	8,57	31,06	-	36,20	-
Dynamis [7]	1396	Selexol	90,3	-	-	33,10	-	33,10	-
Dynamis [7]	1396	Selexol	90,2	99,950	3,00	31,30	-	33,10	-

First a comparison between the PSA-based cases is carried out. The case termed *Only power* is the result of a process simulation based on the same composite model used for all other cases reported in this work. It represents the IGCC plant with a single PSA train and without ultrapure H_2 production. This set of results is useful to evaluate the change in performance when coproducing H_2. Two other cases are displayed (*Two-train PSA* and *One-train PSA*), representing the two novel configurations proposed. The instances were selected, among those reported in the previous sections, in order to have similar ultrapure H_2 throughput and, thus, to allow easier comparisons of the results. Whilst the coal input is kept almost constant for the cases involving two products, when the output is only power the coal input has been decreased in order to utilize the same gas turbine working with a similar load factor. In this way, the performance of the gas turbine could not be considered a discriminating factor for different performances.

Coproducing ultrapure H_2 necessarily results in lower η_{el}, since part of the energy is stored in the H_2 (η_{H2}). η^*_{tot} is enhanced when ultrapure H_2 is produced, in both the two configurations analysed. However, the *Two-train PSA* case displays a slightly better energy performance. Another advantage over the *One-train PSA* alternative is the H_2 purity which fully matches the requirement. The CO_2 separation efficiency (represented in the table by R_{CO2}) displays a small increase when moving to a coproduction layout. The *One-train PSA* case returns a R_{CO2} slightly higher than the *Two-train PSA* case. Overall the

differences are very small, about 1%. It must be stressed that a key benefit of implementing a *One-train PSA* configuration cannot be grasped by the table, as it consists in the utilization of a single separation stage instead of two.

If we broaden the comparative analysis also to the selected results from the literature, the advantage of using PSA for both separating CO_2 and purifying H_2 seems to be supported. Overlooking the absolute numbers, which may be influenced by different assumptions, it is meaningful to analyse the relative variations of the performance indicators (given the lack of enough information for calculating η^*_{tot} in all the cases, the cumulative efficiency term considered is η_{tot60}). When coproducing a similar throughput of ultrapure H_2, η_{tot60} tend to increase in all the cases reported. The largest increase is registered with the *Two-train PSA* case (+ 0.61%) followed by the *One-train PSA* case (+ 0.37%). The selected absorption-based literature cases whether report the same value (+ 0%) [7] or a more limited increase (+ 0.18 %) [10]. Even though the complexity of the systems demands caution with comparison of different sets of results, the reported outcome seems to comply with the beneficial effect of avoiding tail gas compression attained with the novel configurations proposed. This energy saving would be more significant the larger the ultrapure H_2 production is compared to the power output. On a CO_2 separation perspective (i.e. CO_2 recovery), the results show that the absorption-based system displays better performance both in an only power and in a coproduction layout. Finally, it is important to point out that the utilization of PSA technology brings along some issues to be addressed. Complexity of the arrangement, possible large footprint and necessity to smooth out fluctuations in the flue gas to the gas turbine are typical examples. The latter issue is stressed when off-design operating conditions apply, like the cases studied in this work [42].

6. Conclusions

Two novel system configurations of an IGCC plant coproducing power and ultrapure H_2 with CO_2 capture are presented. Both are based on PSA technology for separating CO_2 from the shifted syngas and purifying H_2. The main reason for the coproduction of ultrapure H_2 is the possibility to increase the flexibility of the power output. The configurations proposed demonstrated to fulfil this requirement as the output of the plant could be shifted to a certain extent between the two plant products without losing in efficiency. Within the cases reported, a load variation of about 12% (net power output reduced from 348 MW to 305 MW) could be reached by increasing the ultrapure H_2 throughput (up to a maximum of 154 MW) while the coal feeding is maintained constant. Larger load variations are realistically achievable given a minimum redesign of the PSA processes. In this sense PSA does not seem to pose limits in the flexibility achievable. Thereby the power plant has the possibility to effectively comply with the variability of electricity demand, characteristic of paramount importance in view of the future energy market. The first configuration relies on two PSA trains in series and was termed *Two-train PSA*. While the main goal of the first train is CO_2 removal from the shifted syngas, the second train further processes part of the H_2-rich off-gas in order to increase the H_2 purity. The utilization of the same technology allows for an advantageous integration scheme between the two processes. The shift between power output and ultrapure H_2 can be achieved with different strategies, allowing for an interesting potential of flexible operation not fully explored in this paper. The cases reported increased the ultrapure H_2 throughput by augmenting the gas sent to the second PSA process and adjusting the relative cycle scheduling in order to fulfil the process requirements. The units upstream the first PSA are basically unaffected by this procedure and are, thus, able to retain good working efficiencies. Accordingly, the plant energy efficiency is stable on a good level at varying power outputs. The CO_2 separation performance is on acceptable levels and slightly increases with the decrease of the power output. The second configuration assessed consists of a single PSA train and was for this reason termed *One-train*

PSA. The process is able to concentrate CO_2 from the shifted syngas, while producing two H_2-rich gas streams. A first stream characterized by a high H_2 purity (up to 99.99+% vol.) and a second one with a lower H_2 content (82-85%), which constitutes the continuous fuel feed of the gas turbine. Different shares of power and ultrapure H_2 could be obtained by simply modifying the purge-to-feed ratio of the PSA process. The upstream processes are again unaffected by these modifications of the PSA process and can keep on working at their design point. However, issues arose regarding the possibility of achieving very high H_2 purities in all the operating conditions analysed. Only one of the cases reported strictly fulfilled the H_2 purity specification established (99.99+% vol.), which is defined considering PEM fuel cells as final application. If such high purity is required, the flexibility of the plant could not be completely realized. More relaxed purity constraints would enable a high degree of flexibility, with relatively good energy and CO_2 separation performance and an easier plant design (one separation stage instead of two like in all the other alternatives).

In order to complete the overview on the novel PSA-based system configurations, a comparative analysis is carried out with the most common arrangement for power and ultrapure H_2 coproduction in IGCC plants. It consists of an absorption unit for processing the shifted syngas followed by a PSA for further H_2 purification. The related results refer to two studies, selected after a screening of the relevant literature. Introducing the production of ultrapure H_2 appears to be more effective when also the CO_2 separation is carried out through a PSA process, as can be argued by the cumulative efficiency. The main advantage is that PSA technology allows avoiding the power consumption related to PSA tail gas compression, common in the configuration including absorption. Between the two proposed options, the *Two-train PSA* configuration demonstrated to perform better in terms of energy efficiency.

Although the discussed advantages of the novel configurations presented, the general viability has yet to be proven since PSA integration into an IGCC plant has normally a lower overall performance than absorption. It needs to be evaluated if the benefits introduced with ultrapure H_2 coproduction are sufficient to make up for this initial performance gap. The scattering of results in the literature makes this evaluation not straightforward. A possible solution would be to utilize a common modeling framework to assess the performance of both options. Other issues may also arise when adopting PSA technology, among those the need for controlling the fluctuations in the H_2-rich gas rate to the gas turbine due to the PSA cyclic operation. Lastly, this is a very first assessment of such system entirely based on PSA technology. A further optimization is likely feasible, exploiting developments in the processes and in the materials (e.g. adsorbents effectively performing at high temperatures allowing for warm gas cleaning processes). Moreover a simplification of the PSA layout is possible with advantages in terms of footprint. In particular the *Two-train PSA* configuration relies on a fairly complex second PSA cycle, which was developed to obtain high H_2 recovery. Since that is not an important requirement in the case proposed, an easier PSA cycle could be advisable.
In conclusion, the system analysis conducted suggests IGCC plants completely based on PSA as gas separation technology to be rather promising. PSA processes allow shifting between varying power-to-hydrogen ratios without significant energy penalties, increasing so plant flexibility at partial loads.

Acknowledgements

The authors gratefully acknowledge the financial support provided through the Norwegian University of Science and Technology (NTNU).

Nomenclature

a_i	number of neighboring sites occupied by adsorbate molecule for species i
C_i	gas concentration of species i, mol/m^3
$C_{ads,i}$	specific heat of species i in the adsorbed phase, J/(mol K)
$C_{p,G}$	gas specific heat at constant pressure, J/(mol K)
$C_{p,s}$	particle specific heat at constant pressure, J/(kg K)
C_{tot}	total gas concentration, mol/m^3
$C_{v,G}$	gas specific heat at constant volume, J/(mol K)
D	diameter of the adsorption column, m
$D_{ax,i}$	axial dispersion coefficient of species i, m^2/s
d_p	particle diameter, m
$\Delta H_{r,i}$	isosteric heat of adsorption of species i, J/mol
k_i	equilibrium constant of species i, Pa^{-1}
$k_{\infty,i}$	adsorption constant at infinite temperature of species i, Pa^{-1}
$k_{LDF,i}$	linear driving force coefficient of species i, s^{-1}
L	length of the adsorption column, m
P	pressure, Pa
PSA-R_{CO2}	PSA CO_2 recovery
PSA-Y_{CO2}	PSA CO_2 purity
PW/H_2	ratio of net electric output and H_2 power output
q_i^*	equilibrium adsorbed concentration of species i, mol/kg
$\overline{q}_i$	averaged adsorbed concentration of species i, mol/kg
$q_{m,i}$	maximum adsorption capacity of species i, mol/kg
R	universal gas constant, Pa m^3/(mol K)
R_{CO2}	CO_2 recovery
R_{H2}	H_2 recovery
t	step time, s
T	temperature, K
u_s	superficial velocity, m/s
Y_{CO2}	CO_2 purity
Y^*_{H2}	ultrapure H_2 purity

Greek letters

ε	bed void fraction
ε_p	particle void fraction
η_{el}	net electric efficiency
$\eta_{el\ prod}$	power production efficiency
η_{H2}	hydrogen efficiency
η_{tot60}	converted cumulative efficiency (with a factor 0.6)
η^*_{tot}	converted cumulative efficiency (with a factor $\eta_{el\ prod}$)
λ_{ax}	axial thermal dispersion coefficient, J/(s m K)
ρ_G	gas volumetric mass density, kg/m^3
ρ_p	particle volumetric mass density, kg/m^3

Subscripts

i	species

Superscripts

NC number of components

References

1. IPCC, *Climate Change 2014: Synthesis Report.*, 2014, IPCC: Geneva, Switzerland. p. 151 pp.
2. IEA, *Energy and Climate Change - World Energy Outlook Special Report*, 2015.
3. IEA, *Technology Roadmap - Carbon capture and storage*, 2013.
4. Brouwer, A.S., et al., *The Flexibility Requirements for Power Plants with CCS in a Future Energy System with a Large Share of Intermittent Renewable Energy Sources.* Energy Procedia, 2013. **37**: p. 2657-2664.
5. IEAGHG, *Operating Flexibility of Power Plants with CCS*, 2012.
6. Jansen, D., et al., *Pre-combustion CO2 capture.* International Journal of Greenhouse Gas Control, 2015. **40**: p. 167-187.
7. DYNAMIS, *Towards Hydrogen and Electricity Production with Carbon Dioxide Capture and Storage*, 2009.
8. Kreutz, T., et al., *Co-production of hydrogen, electricity and CO2 from coal with commercially ready technology. Part B: Economic analysis.* International Journal of Hydrogen Energy, 2005. **30**(7): p. 769-784.
9. Chiesa, P., et al., *Co-production of hydrogen, electricity and CO2 from coal with commercially ready technology. Part A: Performance and emissions.* International Journal of Hydrogen Energy, 2005. **30**(7): p. 747-767.
10. Cormos, C.-C., *Assessment of hydrogen and electricity co-production schemes based on gasification process with carbon capture and storage.* International Journal of Hydrogen Energy, 2009. **34**(15): p. 6065-6077.
11. Cormos, C.-C., *Evaluation of energy integration aspects for IGCC-based hydrogen and electricity co-production with carbon capture and storage.* International Journal of Hydrogen Energy, 2010. **35**(14): p. 7485-7497.
12. Davison, J., et al., *Co-production of hydrogen and electricity with CO2 capture.* International Journal of Greenhouse Gas Control, 2010. **4**(2): p. 125-130.
13. Chen, Q., A. Rao, and S. Samuelsen, *H2 coproduction in IGCC with CCS via coal and biomass mixture using advanced technologies.* Applied Energy, 2014. **118**: p. 258-270.
14. Li, M., A.D. Rao, and G. Scott Samuelsen, *Performance and costs of advanced sustainable central power plants with CCS and H2 co-production.* Applied Energy, 2012. **91**(1): p. 43-50.
15. Cormos, C.-C., *Hydrogen and power co-generation based on coal and biomass/solid wastes co-gasification with carbon capture and storage.* International Journal of Hydrogen Energy, 2012. **37**(7): p. 5637-5648.
16. Cormos, C.-C., F. Starr, and E. Tzimas, *Use of lower grade coals in IGCC plants with carbon capture for the co-production of hydrogen and electricity.* International Journal of Hydrogen Energy, 2010. **35**(2): p. 556-567.
17. Ahn, S., et al., *Layered two- and four-bed PSA processes for H2 recovery from coal gas.* Chemical Engineering Science, 2012. **68**(1): p. 413-423.
18. Lopes, F.V.S., C.A. Grande, and A.E. Rodrigues, *Activated carbon for hydrogen purification by pressure swing adsorption: Multicomponent breakthrough curves and PSA performance.* Chemical Engineering Science, 2011. **66**(3): p. 303-317.
19. Ribeiro, A.M., et al., *A parametric study of layered bed PSA for hydrogen purification.* Chemical Engineering Science, 2008. **63**(21): p. 5258-5273.
20. Ribeiro, A.M., et al., *Four beds pressure swing adsorption for hydrogen purification: Case of humid feed and activated carbon beds.* AIChE Journal, 2009. **55**(9): p. 2292-2302.
21. Sircar, S. and T.C. Golden, *Purification of Hydrogen by Pressure Swing Adsorption.* Separation Science and Technology, 2000. **35**(5): p. 667-687.

22. Luberti, M., et al., *Design of a H2 PSA for cogeneration of ultrapure hydrogen and power at an advanced integrated gasification combined cycle with pre-combustion capture.* Adsorption, 2014. **20**(2-3): p. 511-524.
23. Riboldi, L. and O. Bolland, *Evaluating Pressure Swing Adsorption as a CO2 separation technique in coal-fired power plants.* International Journal of Greenhouse Gas Control, 2015. **39**(0): p. 1-16.
24. Riboldi, L. and O. Bolland, *Comprehensive analysis on the performance of an IGCC plant with a PSA process integrated for CO2 capture.* International Journal of Greenhouse Gas Control, 2015. **43**: p. 57-69.
25. Liu, Z. and W.H. Green, *Analysis of Adsorbent-Based Warm CO2 Capture Technology for Integrated Gasification Combined Cycle (IGCC) Power Plants.* Industrial & Engineering Chemistry Research, 2014. **53**(27): p. 11145-11158.
26. Gazzani, M., E. Macchi, and G. Manzolini, *CO2 capture in integrated gasification combined cycle with SEWGS – Part A: Thermodynamic performances.* Fuel, 2013. **105**(0): p. 206-219.
27. Manzolini, G., et al., *Integration of SEWGS for carbon capture in Natural Gas Combined Cycle. Part B: Reference case comparison.* International Journal of Greenhouse Gas Control, 2011. **5**(2): p. 214-225.
28. Baade, W., et al., *CO2 capture from SMRs: A demonstration project.* Hydrocarbon Processing, 2012: p. 63-68.
29. Sircar, S. and W.C. Kratz, *Simultaneous Production of Hydrogen and Carbon Dioxide from Steam Reformer Off-Gas by Pressure Swing Adsorption.* Separation Science and Technology, 1988. **23**(14-15): p. 2397-2415.
30. Alptekin, G.D., Steve; Jayaraman, Ambal; Dubovik, Margarita; Amalfitano, Robert;. *A Low Cost, High Capacity Regenerable Sorbent for CO2 Capture*. in *A&WMA's 102nd annual conference & exhibition*. 2009.
31. Alptekin, G.J., Ambalavanan; Copeland, Robert; Dietz, Steve; Bonnema, Michael; Schaefer, Matt; Cesario, Michael, *Novel warm gas CO2 capture technology for IGCC power plants*, 2013, TDA Research Inc.
32. *DECARBit: Enabling advanced pre-combustion capture techniques and plants. European best practice guidelines for assessment of CO2 capture technologies*, 2011, European Benchmarking Task Force.
33. Riboldi, L. and O. Bolland, *Determining the potentials of PSA processes for CO2 capture in Integrated Gasification Combined Cycle (IGCC).* In press. Energy Procedia, 2015.
34. *Thermoflex Version 24.0.1*, 2014, Thermoflow Inc.
35. *gPROMS 4.1.0*, 2015, Process System Enterprise Limited.
36. *Aspen HYSYS V7.3*, 2011, Aspen Technology Inc.
37. Lopes, F.V.S., et al., *Adsorption of H2, CO2, CH4, CO, N2 and H2O in Activated Carbon and Zeolite for Hydrogen Production.* Separation Science and Technology, 2009. **44**(5): p. 1045-1073.
38. IEA, *Power Generation from Coal: Measuring and Reporting Efficiency Performance and CO2 emissions.*, 2010.
39. de Visser, E., et al., *Dynamis CO2 quality recommendations.* International Journal of Greenhouse Gas Control, 2008. **2**(4): p. 478-484.
40. Siriwardane, R.V., et al., *Adsorption of CO2 on Molecular Sieves and Activated Carbon.* Energy & Fuels, 2001. **15**(2): p. 279-284.
41. Ahn, H., J. Yang, and C.-H. Lee, *Effects of Feed Composition of Coke Oven Gas on a Layered Bed H2 PSA Process.* Adsorption, 2001. **7**(4): p. 339-356.
42. Najmi, B., O. Bolland, and K.E. Colombo, *Load-following performance of IGCC with integrated CO2 capture using SEWGS pre-combustion technology.* International Journal of Greenhouse Gas Control, 2015. **35**(0): p. 30-46.